Synthesis and Characterization of Tanninsulfonic Acid Doped Polyaniline–Metal Oxide Nanocomposites

Venu Gopal Bairi,[1] Brock A. Warford,[1] Shawn E. Bourdo,[1,2] Alexandru S. Biris,[2] Tito Viswanathan[1]

[1]*Department of Chemistry, University of Arkansas at Little Rock, 2801 South University Avenue, Little Rock, Arkansas 72204*
[2]*University of Arkansas at Little Rock Nanotechnology Center, University of Arkansas at Little Rock, 2801 South University Avenue, Little Rock, Arkansas 72204*

Received 22 February 2011; accepted 9 July 2011
DOI 10.1002/app.35242
Published online 21 November 2011 in Wiley Online Library (wileyonlinelibrary.com).

ABSTRACT: Composites of conducting polymers and metal oxides have a potential role in electronic devices because of their enhanced physical and electronic properties. An *in situ* synthesis of metal oxide nanocomposites of polyaniline (PANI) and tanninsulfonic acid doped PANI was carried out at −10°C with two different ratios of aniline to sodium persulfate (oxidant) and the simultaneous incorporation of TiO_2, Al_2O_3, and ZnO nanopowders. The products were characterized by X-ray diffraction (XRD), thermal analysis, spectroscopy, and electrical conductivity measurements. XRD and thermogravimetric analysis confirmed the presence of the metal oxide in the final product, whereas the spectroscopic characterization revealed interactions among the tannin, metal oxides, and PANI. The electrical properties were determined by four-point-probe bulk conductivity measurements. © 2011 Wiley Periodicals, Inc. J Appl Polym Sci 124: 3320–3328, 2012

Key words: conducting polymers; infrared spectroscopy; nanocomposites, thermogravimetric analysis (TGA), UV–vis spectroscopy

INTRODUCTION

Intrinsically conducting polymer thin films have been used in various kinds of electronic devices. Conducting polymers are combined with metal oxides because of their enhanced physical and electronic properties and find useful applications in various devices, such as sensors, electrodes, batteries, and photovoltaics.[1,2] Conducting-polymer-based solar cells have gained much importance in the last decade because of their low cost, easy processability, low toxicity, and high environmental stability.[3,4] Among conducting polymers, polyaniline (PANI) is unique because it can be easily doped with various acids and it also exhibits good thermal and environmental stabilities.[5] Metal oxides can also replace fullerenes (electron-acceptor materials) in bulk heterojunction solar cells because of their high electron mobilities.[1,2]

Intrinsically conducting polymers and metal oxides have been used in two ways: as polymer fillings in the voids in thin layers of metal oxide and in *ex situ* blends of polymers and metal oxides to create bulk heterojunctions.

The latter has been found to be more effective as it gives a better photovoltaic response.[6,7] Earlier work has reported the use of the TiO_2 and ZnO nanoparticles, which have good electron mobility, thermal stability, and electron-acceptor properties for use in solar cell applications.[6,8]

Here, we synthesized these nanocomposites by an *in situ* synthetic method, which could replace the aforementioned *ex situ* preparations. The characterization of these *in situ* prepared products was carried out to determine if the metal oxides could be incorporated successfully and to study the properties of the polymer–metal oxide nanocomposites. The tanninsulfonic acid doped polyaniline (TANIPANI) composites synthesized by this *in situ* method was found to have different electronic properties than the PANI nanocomposites. The tanninsulfonic acid in this reaction acted as a dopant, whereas the free hydroxyl groups on the tannin increased the solubility of TANIPANI by forming hydrogen bonds with the solvent.[9] The *o*-catechol (*o*-dihydroxyphenyl) group on the tannin helped in the complexation of the metal ions.[10] TANIPANI could be used as a potential heterojunction material for use in solar cells.[11]

Many techniques, including the sol–gel method, inverted emulsion polymerization,[12] and ultrasonic

Additional Supporting Information may be found in the online version of this article.

Correspondence to: V. G. Bairi (vxbairi@ualr.edu) or T. Viswanathan (txviswanatha@ualr.edu).

Contract grant sponsor: U. S Department of Energy; contract grant number: DE-FG 36-06 GO 86072.

irradiation,[13] have been used for the preparation of these polymer–metal oxide nanocomposites. Here, we report the general method of synthesis of these composites at −10°C as per the method of MacDiarmid et al.;[14] we used isopropyl alcohol as the reaction solvent, which prevented the freezing of the reaction contents. X-ray diffraction (XRD) and thermogravimetric analysis (TGA) confirmed the presence of metal oxides in the final product. Spectroscopic methods were used to determine the structural and electronic properties. The electrical conductivities of the samples were analyzed with respect to the reaction conditions and metal oxide content.

EXPERIMENTAL

Materials

Aniline, obtained from Fisher Scientific Co., (Fair Lawn, New Jersey) was double-distilled before use. Methanesulfonic acid (70%), obtained from Aldrich Chemicals (Milwaukee, WI), was diluted to a 1*M* solution. Ammonium hydroxide (ACS reagent grade, 28–30%), obtained from Sigma-Aldrich (St. Louis, MO) was diluted to a 1M solution. *m*-Cresol (99%), 1-methyl-2-pyrrolidinone (NMP; 99%), and sodium persulfate (reagent grade, ≥98%), obtained from Sigma-Aldrich (St. Loius, MO), were used as received. 10-Camphorsulfonic acid (98%), titanium dioxide nanopowder (average particle size = 21 nm, 99.5% purity), aluminum oxide nanopowder (average particle size = 13 nm, ≥99.8% purity), and ZnO (6% Al-doped nanopowder, <50 nm, brunauer emmett teller (BET), 97% purity), obtained from Aldrich Chemicals (St. Louis, MO), were used as received. Sulfonated tannin (d3 form) was obtained from Chevron Philips (Bartlesville, OK).

Synthesis procedure

The TANIPANI–metal oxide nanocomposites were synthesized by the oxidative polymerization of aniline, as described by MacDiarmid et al.,[14] in the presence of isopropyl alcohol to prevent the freezing of the reaction contents at low temperatures. A 120-mL aliquot of 1*M* methanesulfonic acid was added to a jacketed beaker. A specific mass aliquot of tanninsulfonate and metal oxide (Al_2O_3, TiO_2, or ZnO) was added to the reaction mixture to give an approximate metal oxide content of 10% in the final product. After all of the contents were dispersed in the aqueous acid, 2 mL of aniline was added; this was followed by the addition of 80 mL of isopropyl alcohol. The reaction temperature was brought down to −10°C. Sodium persulfate (at two different molar ratios to aniline) was dissolved in 40 mL of methanesulfonic acid and added to the reaction mixture dropwise. The reaction was filtered when the contents of the reaction mixture turned green. The precipitate was washed thoroughly with deionized water until the filtrate was colorless; this was followed by washing with 50 mL of methanesulfonic acid. A small amount of this doped product (emeraldine salt) was collected for characterization studies. The remaining product was dedoped (emeraldine base) by stirring in 0.1*M* ammonium hydroxide to wash away all of the methanesulfonic acid used in the polymerization reaction. All of the products were dried in a vacuum oven.

Characterization methods

XRD studies were made on the dedoped powdered samples with a Bruker D8-Discover instrument (Madison, WI).

TGA of the dedoped powder samples was performed with a Mettler-Toledo TG50 (Greifensee, Switzerland) instrument by heating the sample from 35 to 850°C at a rate of 10°C/min in the presence of air flow. TGA was used to determine the amount of metal oxides in the samples and to analyze the thermal stability of the composites.

Ultraviolet–visible (UV–vis) spectroscopy was performed with a PerkinElmer UV–vis/near infrared spectrometer (Norwalk, CT). The spectra of the film forms of the doped samples and dedoped samples in NMP were recorded. Dedoped product from this experiment was doped with camphorsulfonic acid (1 : 2 mol/mol mixture of emeraldine base to camphor sulfonic acid). The mixture was dissolved in *m*-cresol, and the solution was spin-cast on a glass slide at 800 rpm. The films were dried at 70°C for 2 h.

Fourier transform infrared (FTIR) spectra of the dedoped samples in KBr pellets were recorded with a Nicolet Magna-IR 550 spectrometer (Madison, WI).

The conductivities were measured with a colinear four-point probe method on pellets with a Keithley 224 programmable current source and a Keithley 617 electrometer (Cleaveland, OH). Pellets for the conductivity studies were made by the pressing of the doped PANI at 15,000 psi with a Carver hydraulic press.

RESULTS AND DISCUSSION

XRD studies

To confirm the presence of metal oxides in the composites, the XRD patterns were analyzed. The diffraction peaks that resulted from the base form of PANI were evident at 15, 18, and 22° values of 2θ because of the stacking of the individual chains.[15] The peaks were more distinct in case of PANI (compared to TANIPANI); this indicated that PANI was more crystalline in nature, as shown in Figure 1.

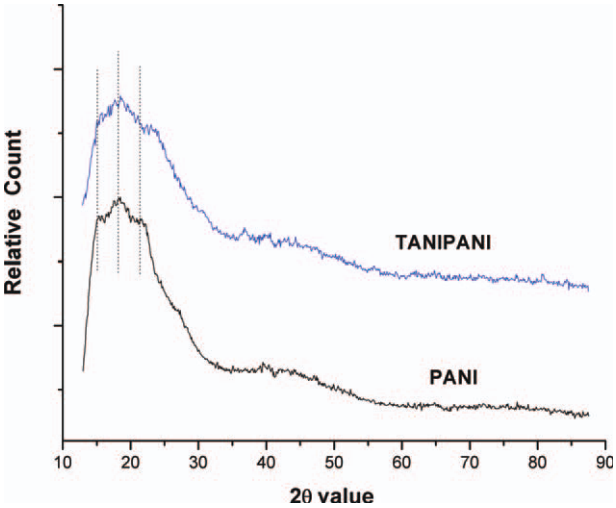

Figure 1 XRD patterns of PANI and TANIPANI. [Color figure can be viewed in the online issue, which is available at wileyonlinelibrary.com.]

Figure 2(a,b) shows that additional peaks were present in the samples containing Al_2O_3 and TiO_2. Peaks for the metal oxides of TiO_2 and Al_2O_3 were present, but no distinct peaks were evident for the ZnO; this indicated that ZnO was probably not incorporated in the polymer nanocomposites. ZnO may have formed some soluble salts in the reaction, which were washed away during the filtration. TiO_2 was present in the anatase and rutile forms: the peaks at 24.9, 36.8, 37.7, 47.7, 53.7, and 62.7° in XRD were characteristic of the anatase form of TiO_2, indicated by the letter a, whereas the peaks at 27, 36, 41.1, and 54.68° were characteristic of the rutile form, indicated by the letter r, as shown in Figure 2.[16] The characteristic diffraction patterns of Al_2O_3 were observed at 34.7, 36.9, 39.4, 45.38, and 67°.[5] The average particle sizes could be calculated from the Scherrer equation:

$$L = \lambda K/\beta \cos\theta$$

where L is the average particle size, $\lambda = 0.1540$ nm and is the wavelength of the laser, $K = 0.9$ and is the Scherrer constant, β is the maximum width at half of the peak height (rad), and θ is the value of the angle at peak height.

The crystallite sizes for TiO_2 and Al_2O_3 were found to be in the ranges 15–18 and 6–8 nm, respectively, whereas the particle sizes were found to be 21 nm and less than 13 nm. This indicated that the particles were made up of very few individual crystallites. The data presented in Table I give the crystallite sizes for the most intense peak position.

TGA

XRD analysis confirmed the presence of TiO_2 and Al_2O_3, and the thermograms in Figure 3(a,b) indicate about 7–15% of TiO_2 and Al_2O_3 existed in the nanocomposites. From the thermograms in Figure 3(a,b), it was evident that ZnO was not incorporated into the polymer under these conditions, and this confirmed the results from XRD. TGA, along with the XRD data, indicated the incorporation of TiO_2 and Al_2O_3, and the amount of metal oxides left are shown in Table II.

TANIPANI and PANI differed significantly with respect to weight loss in certain temperature regions of the thermogram, as shown in Figure 4. From 120 to 310°C, the weight loss in TANIPANI was about

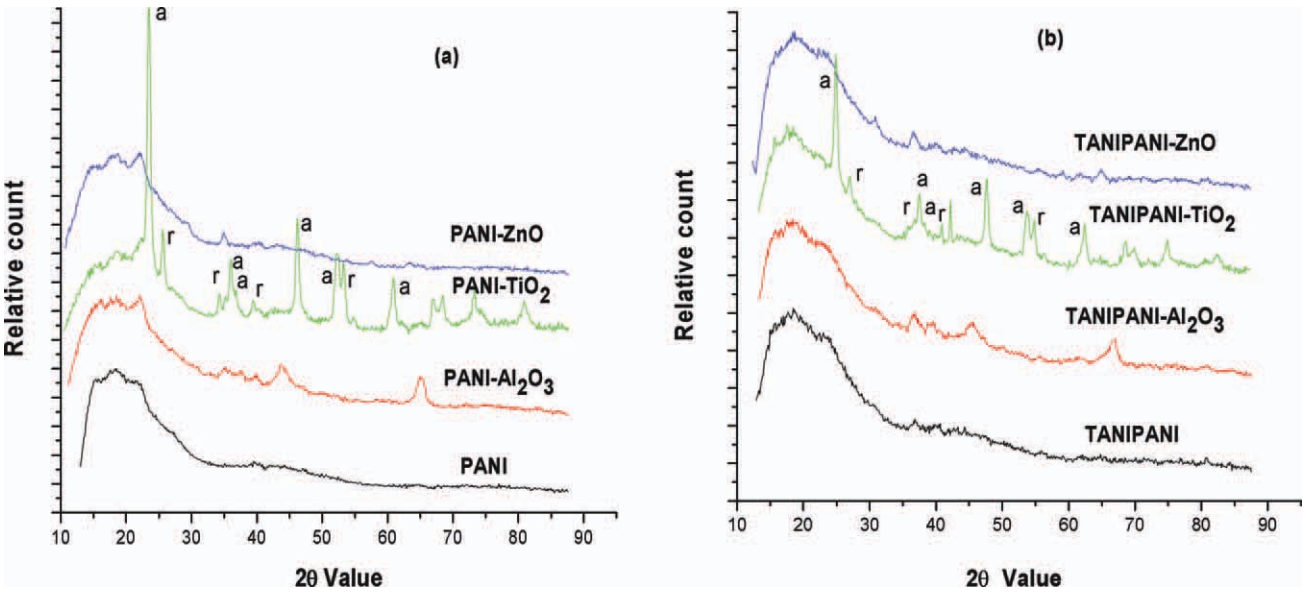

Figure 2 XRD patterns of the (a) PANI–metal oxide nanocomposites and (b) TANIPANI–metal oxide nanocomposites. [Color figure can be viewed in the online issue, which is available at wileyonlinelibrary.com.]

TABLE I
Average Particle Sizes of the Metal Oxides, Calculated from the X-Ray Diffractograms with the Scherrer Equation

Sample	θ (peak position)	λK	$\beta \cos \theta$	L (nm)
PANI–TiO_2	23.4	1.3865	0.0088	15.74
PANI–TiO_2	25.6	1.3865	0.0062	22.02
TANIPANI–TiO_2	24.9	1.3865	0.0085	16.22
TANIPANI–TiO_2	27	1.3865	0.0077	17.83
PANI–Al_2O_3	32.4	1.3865	0.0206	6.72
PANI–Al_2O_3	21.9	1.3865	0.0210	6.58
TANIPANI–Al_2O_3	45.3	1.3865	0.0193	7.17
TANIPANI–Al_2O_3	39.6	1.3865	0.0213	6.49

2.3%, whereas that in PANI was 0.7%. TANIPANI degraded completely at 700°C, whereas PANI degraded completely at 650°C. From the first derivatives of the PANI and TANIPANI thermograms, it was apparent that TANIPANI had a broad degradation curve and a shoulder at 650°C; this was not found in PANI. For each ratio of oxidant to monomer, the thermograms were similar; therefore, we displayed only a representative set from the samples synthesized with a 1 : 1 molar ratio of aniline to oxidant.

The thermal stability of TANIPANI was lower compared to that of PANI alone. The low onset degradation temperature for TANIPANI was not surprising because of the oxygen atoms in the tannin molecule, which may have promoted the faster degradation of the polymer. These results were also consistent with TANIPANI being amorphous in nature compared to PANI in the XRD studies. With the incorporation of metal oxides, the thermal stability of PANI was found to increase, as shown in Figure 5. (This indicated that there was some interaction between the metal oxides and PANI/TANIPANI.)

UV–vis characterization

UV–vis spectroscopy was helpful in determining the interaction of tannin and metal oxides with PANI. Two absorption bands for the dedoped PANI were evident at 327 and 639 nm; these resulted from the π–π* transition of the conjugated ring system and the benzenoid to quinoid transition, respectively.[17] Tannin alone exhibited an absorption band around 286 nm, as shown in Figure 6. The dedoped TANIPANI spectra gave an absorption band at 327 nm with a shoulder at 285 nm. The absorption increased and became very noisy at a wavelength lower than the π–π* in PANI but not in TANIPANI, as shown in Figure 6. This modulation of the absorption spectrum indicated a change in the electronic properties, and modulation resulted from the bonding between the tannin molecule and the PANI backbone.

Instead of two distinct peaks for the tannin and PANI, a single broad peak in the region 260–320 nm was observed, as shown in Figure 7(b); this suggested the chemical bonding of tannin to PANI. The sharp downturn in the UV–vis spectrum of the TANIPANI nanocomposites was attributed to the bonding of the tannin to PANI. The tannin had an absorption band at 285 nm, as shown in Figure 6. The dropdown of the peak below 285 nm in all of the nanocomposites was attributed to tannin. The spectra of PANI with metal oxides also displayed interesting features. It was evident that the

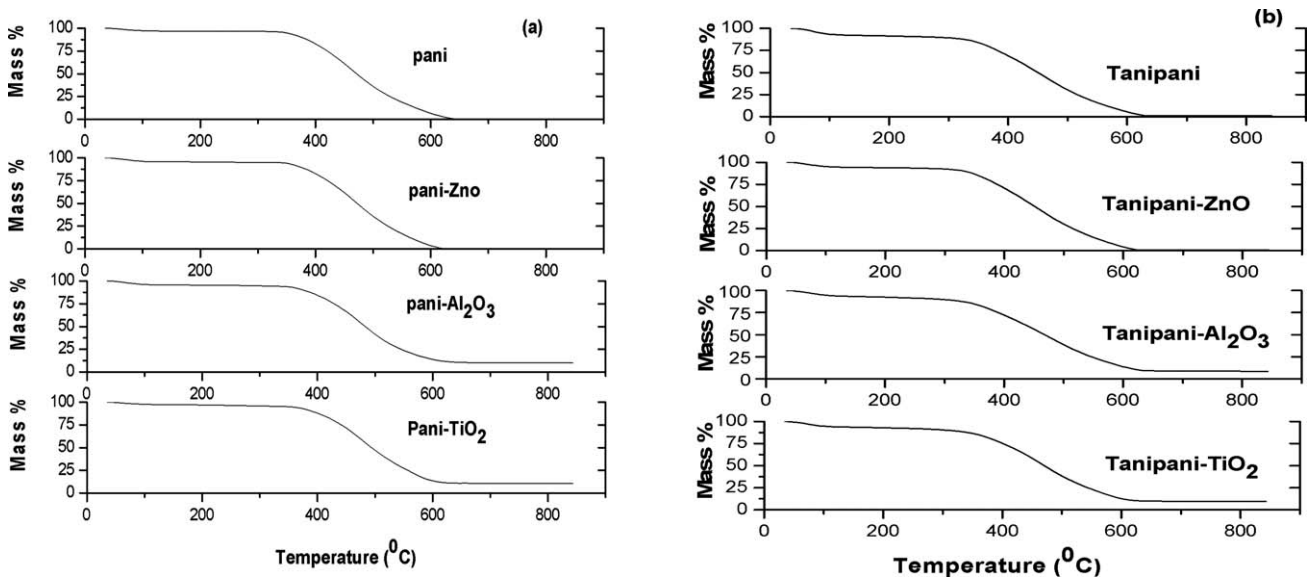

Figure 3 Thermograms showing the degradation of the (a) PANI–metal oxide nanocomposites and (b) TANIPANI–metal oxide nanocomposites.

TABLE II
Percentage of Metal Oxides Left after the Thermal Analysis of the Composites

Sample	Aniline–oxidant ratio	Metal oxide left (%)
PANI–TiO_2	5 : 1	10.6
PANI–TiO_2	1 : 1	14.1
PANI–Al_2O_3	5 : 1	9.8
PANI–Al_2O_3	1 : 1	13.8
TANIPANI–TiO_2	5 : 1	7.6
TANIPANI–TiO_2	1 : 1	15.0
TANIPANI–Al_2O_3	5 : 1	6.2
TANIPANI–Al_2O_3	1 : 1	14.1

absorption band at 327 nm had a better defined peak in the PANI–metal oxide composites than in PANI alone (this indicated the interaction of the metal oxides with PANI), as shown in Figure 7(a).

Because a potential use of these composites is as films in electronic devices, the materials were processed into their doped (electrically conductive) form and cast into films. The spectra of all of the doped PANI composites gave a peak at 420 nm due to the polaron–π^* transition and a free carrier tail, which indicated the electron delocalization in the polymer, as shown in Figure 8(a). In Figure 8(b), we observed a new transition at 800 nm in all of the spectra of the TANIPANI composites due to the π–polaron transition; this indicated the formation of a localized polaron band in TANIPANI. This band was also observed with the PANI–Al_2O_3 and PANI–TiO_2 composites. The results from the UV–vis studies indicate an electronic interaction between PANI and the metal oxide; this was attributed to a coordination bond between the amine nitrogen lone pair of electrons and empty *d* orbitals of the metal.[17] The doped spectra of the TANIPANI–metal oxide nanocomposites showed a very negligible peak at 285 nm, as shown in Figure 8(b); this indicated the presence of tannin, even after processing into films.

IR characterization

The FTIR analysis showed the characteristic vibrational bands for the emeraldine base form of PANI, as shown in Figures 9 and 10. We show only the results of the PANI synthesized from a 1 : 1 molar ratio of aniline to oxidant, as PANI synthesized from a 5 : 1 molar ratio of aniline to oxidant had a similar spectral response. We do not show the data of the ZnO nanocomposites in Table III because ZnO did not get incorporated in the synthesis. Table III displays the information about the different vibrational bands in the PANI nanocomposites synthesized with a 1 : 1 molar ratio of aniline to oxidant.

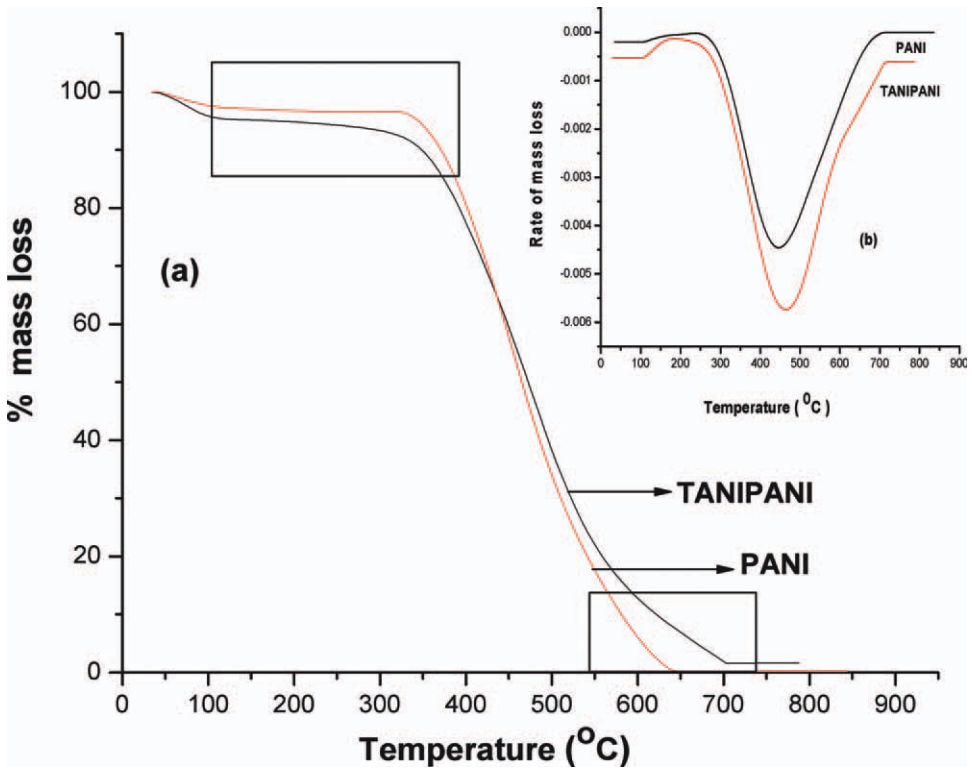

Figure 4 Thermograms showing the (a) thermal decomposition of PANI and TANIPANI and (b) rate of mass loss of PANI and TANIPANI with respect to temperature. [Color figure can be viewed in the online issue, which is available at wileyonlinelibrary.com.]

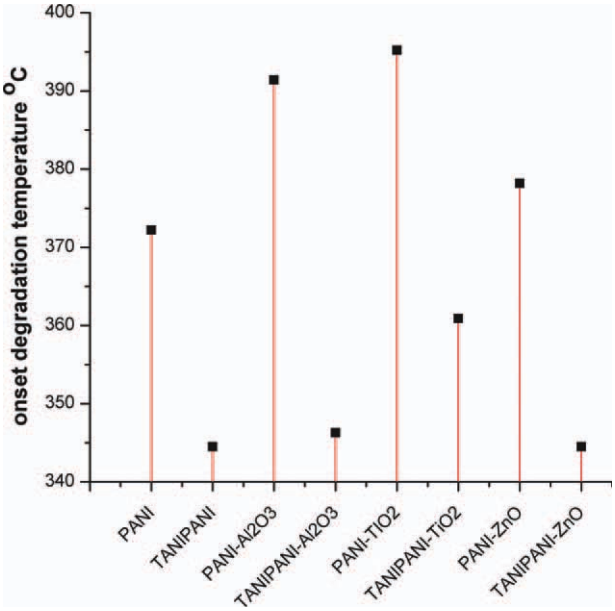

Figure 5 Onset of thermal degradation of various composites of PANI and TANIPANI. [Color figure can be viewed in the online issue, which is available at wileyonlinelibrary.com.]

All of the composites exhibited a broad peak at 3400 cm^{-1} due to the N—H stretching mode; this confirmed the absence of the pernigraniline base form of PANI. The bands at 1580 and 1490 cm^{-1} in all of the spectra indicated that PANI was in the emeraldine form (quinoid–benzenoid at a 1 : 3 ratio).[18,19] These were characteristic bands of emeraldine base due to the quinoid and benzenoid ring stretching vibrations, respectively.

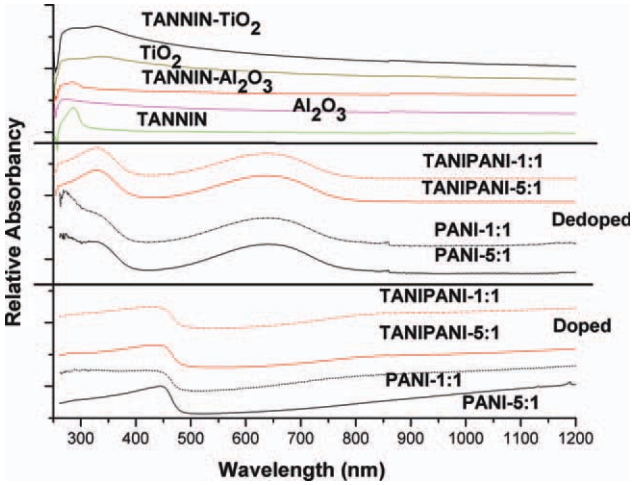

Figure 6 UV–vis spectra of doped and dedoped PANI and TANIPANI and the spectra of the tannin and metal oxides in NMP solvent. [Color figure can be viewed in the online issue, which is available at wileyonlinelibrary.com.]

Because of the interaction of a nitrogen lone pair of electrons with the metal oxides, there was a change in the dipole moment of the C—N bonds (1295 and 1155 cm^{-1}).[20] This change in the dipole moment was evidenced by the shift in the peak positions of the respective C—N stretching vibrations (1295 and 1155 cm^{-1}) toward the higher wave numbers in the case of the polymer nanocomposites containing metal oxides, as shown in Figures 9 and 10. The peak at 1155 cm^{-1} was broad in case of PANI and PANI–ZnO but much sharper in case of PANI–TiO_2 and PANI–Al_2O_3 composites. A similar kind of observation was made with the 823-cm^{-1} peak. The

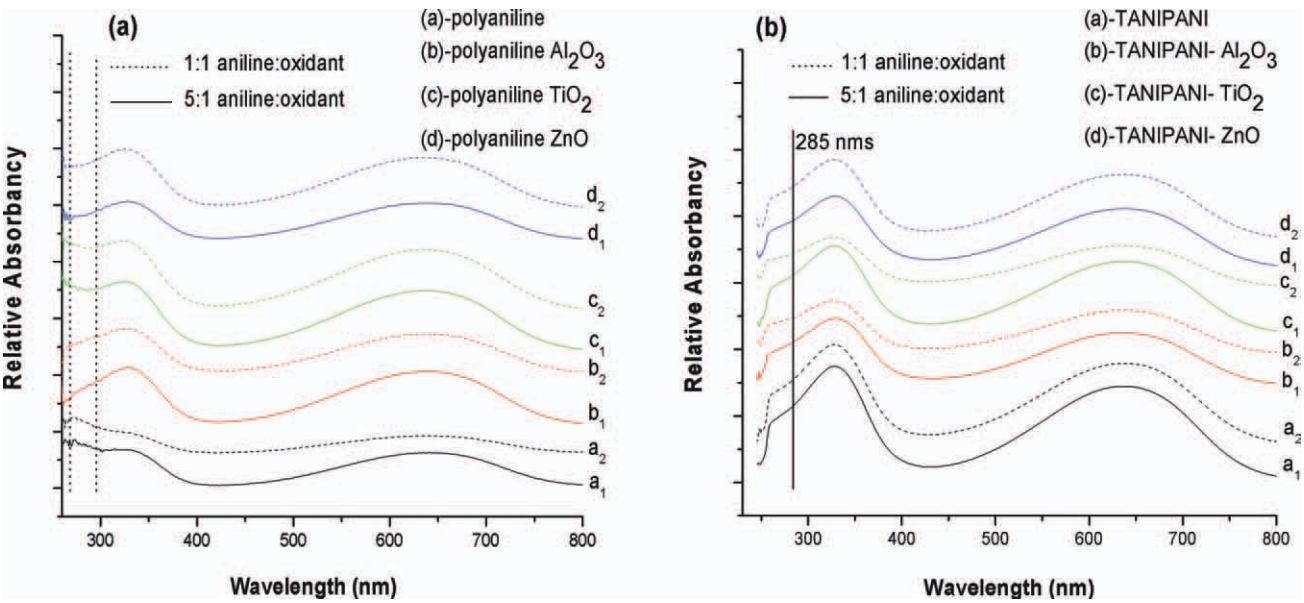

Figure 7 UV–vis spectra of the dedoped (a) PANI–metal oxide nanocomposites and (b) dedoped TANIPANI–metal oxide nanocomposites, both in NMP solvent. [Color figure can be viewed in the online issue, which is available at wileyonlinelibrary.com.]

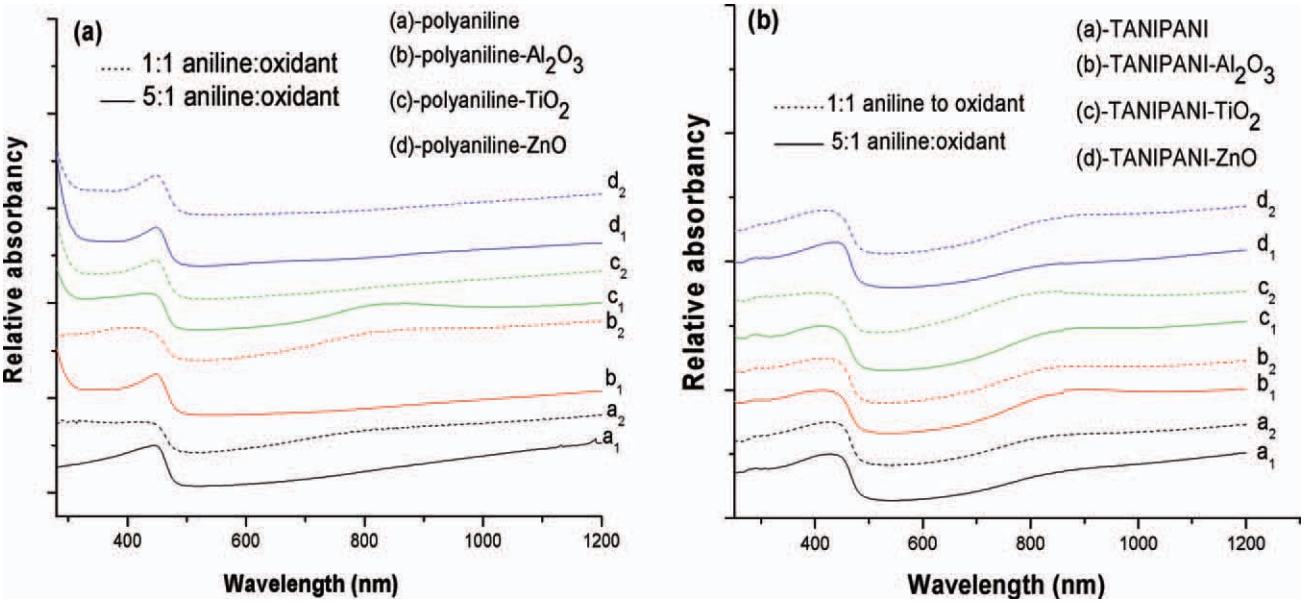

Figure 8 UV–vis spectra of the doped (a) PANI–metal oxide nanocomposites and (b) TANIPANI–metal oxide nanocomposites, both in *m*-cresol solvent. [Color figure can be viewed in the online issue, which is available at wileyonlinelibrary.com.]

changes were more evident in the PANI nanocomposites than in the TANIPANI nanocomposites; this may have been due to the influence of tannin. It was hard to compare the spectra of metal oxides with the spectra of the nanocomposites, as spectral bands for the metal oxides were not very evident in the case of the nanocomposites. This may have been due to the low amount of metal oxide (<15%) incorporated into the PANI nanocomposites, as determined by TGA.

The peak at 1150 cm^{-1} was due to the C—N stretching vibrations in the polymer chains; this was attributed to the electron delocalization. As shown in Figure 9, the peak at 1150 cm^{-1} was more prominent in PANI than in TANIPANI; this may have been related to the higher conductivity of PANI compared to TANIPANI.[21] Para linkages in the polymer chain could be deduced by a strong peak at 825 cm^{-1} in all of the nanocomposites of PANI; this indicated the linearity of the PANI chain.[19]

The sulfonate peak at 1030 cm^{-1} was evident only in the case of TANIPANI but not in PANI, we also observe this peak in all TANIPANI composites but not in PANI composites, as shown in Figures 10

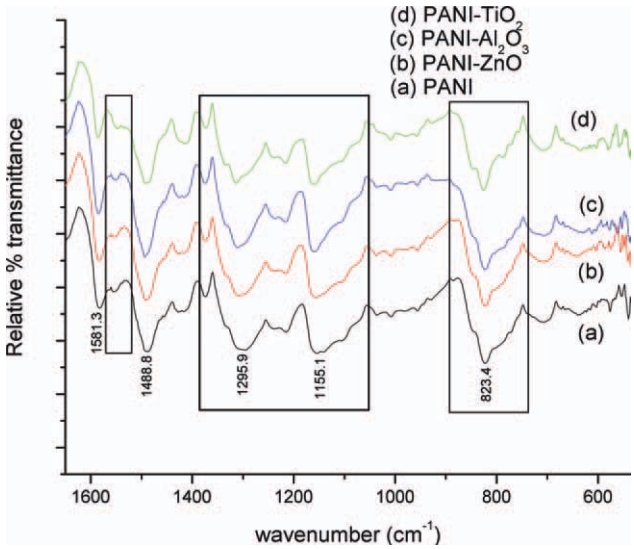

Figure 9 FTIR spectra of the dedoped PANI–metal oxide nanocomposites. [Color figure can be viewed in the online issue, which is available at wileyonlinelibrary.com.]

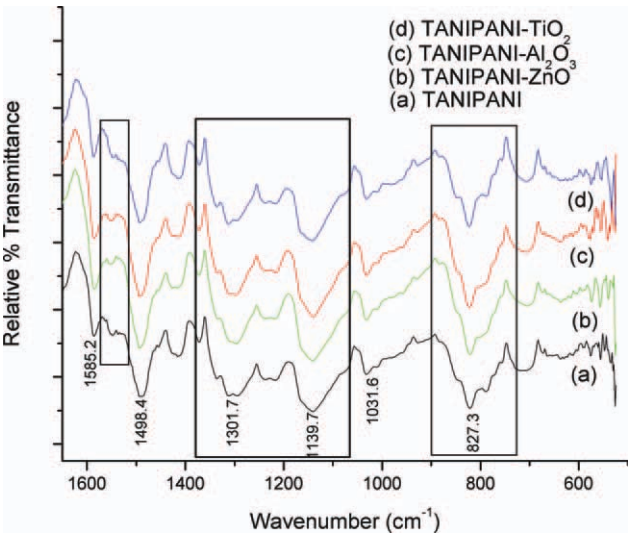

Figure 10 FTIR spectra of the dedoped TANIPANI–metal oxide nanocomposites. [Color figure can be viewed in the online issue, which is available at wileyonlinelibrary.com.]

TABLE III
Band Assignments for Different Vibrations in PANI

Band characteristic	PANI	TANIPANI	PANI–Al_2O_3	TANIPANI–Al_2O_3	PANI–TiO_2	TANIPANI–TiO_2
Stretching vibrations of the quinoid ring	1581.3	1585.2	1585.2	1585.2	1585.2	1587.2
Stretching vibration of the benzenoid ring	1488.8	1498.4	1494.5	1488.8	1492.6	1490.7
*C—N stretching in the secondary amine	1295.9	1301.7	1309.4	1311.3	1313.3	1311.3
*C—N stretching in the quinoid ring	1155.1	1139.7	1159	1139.7	1159	1141.6
Para-disubstituted benzene	823.4	827.3	823.4	821.5	825.3	823.4
C—H out-of-plane bending vibrations	539.9		538/534.9	534.1	538/534.1	534.1

and 11. Because all of the methanesulfonic acid was washed away during dedoping, we did not see any sulfonate peak in PANI alone. Tanninsulfonate was not washed away during dedoping; this was evidenced by the sulfonate peak in the TANIPANI spectra, which indicated the formation of covalent bonds between the tannin and PANI.[9]

Conductivity measurements

The electronic properties were determined by measurement of the conductivity of these nanocomposites. We measured the conductivity values by taking an average of eight readings for each pellet; these are shown in Figure 12. TANIPANI had a lower conductivity than PANI in all of the nanocomposites; this may have been due to the insulating nature of tannin and the presence of less crystalline PANI, as previously discussed. The highest conductivity value of 51 S/cm was observed with PANI doped with methanesulfonic acid. PANI synthesized with a 5 : 1 molar ratio of aniline to oxidant had good conductivity values (ca. 48 S/cm). TANIPANI synthesized with a 5 : 1 molar ratio of aniline to oxidant was found to be less conductive than the TANIPANI synthesized with a 1 : 1 molar ratio of aniline to oxidant. This may have been due to the incorporation of a greater amount of tannin in the 1 : 1 final product relative to the amount of PANI formed in the 5 : 1 final product. With the incorporation of metal oxides, the conductivity values of the PANI and TANIPANI were found to decrease; this could have been due to the amorphous and semiconducting nature of these metal oxides. In the case of the ZnO composites of PANI and TANIPANI, the conductivity values were similar to the PANI/TANIPANI. This may have been due to ZnO not being incorporated into the polymer matrix.

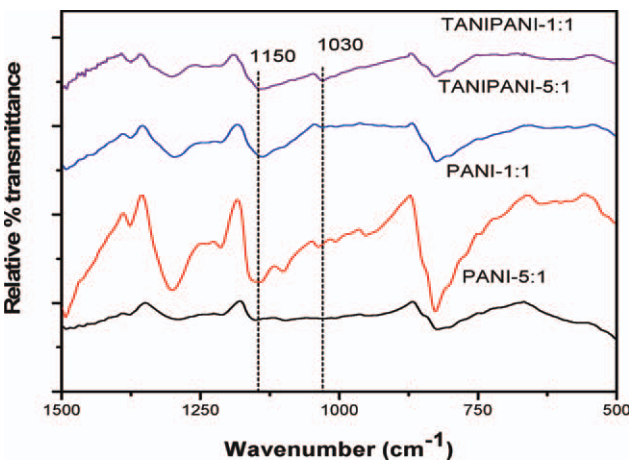

Figure 11 FTIR spectra of the doped PANI showing the peaks of tannin and electron delocalization. [Color figure can be viewed in the online issue, which is available at wileyonlinelibrary.com.]

CONCLUSIONS

We successfully incorporated TiO_2 and Al_2O_3 into conducting polymer matrices; this resulted in PANI and TANIPANI–metal oxide nanocomposites. The physical and electronic properties of the TANIPANI–metal oxides were different than those of the PANI–metal oxide nanocomposites, as evidenced from XRD, TGA, and UV–vis and FTIR spectroscopy. The incorporation of ZnO was not possible with this kind of synthesis, as evident from TGA and XRD analysis. The chemical bonding of tannin to PANI and the interaction of the metal oxides with PANI/TANIPANI were evident both in the doped and dedoped polymers' UV–vis spectra. Carrying out the reaction at −10°C resulted in the preferable formation of the para-coupled product, as indicated by the IR spectrum of the emeraldine base form of PANI. The TANIPANI–metal oxide composites synthesized by this method had bulk conductivity values less than that of the PANI synthesized by the same method but had comparable values to values elsewhere in the literature. The conductivity of the composites was in the semiconductor range; this indicated their possible use in many potential applications. The *in situ* incorporation of metal oxides into PANI could be used to replace the *ex situ* blending of PANI and metal oxides for use in various applications. Future work in this area includes the use of different ratios of TiO_2 and Al_2O_3 in the preparation of TANIPANI nanocomposites and observation of the changes in the physical

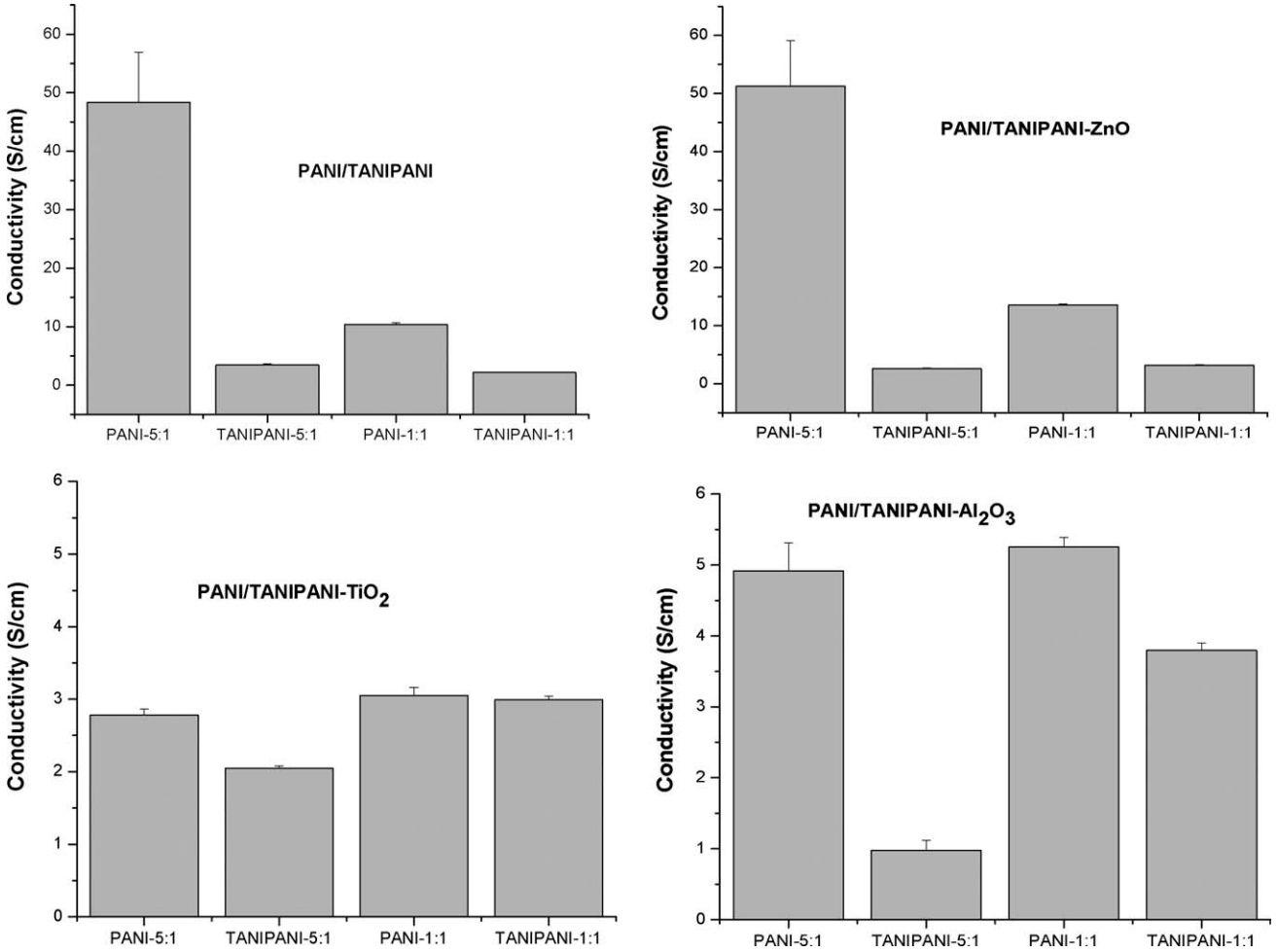

Figure 12 Conductivity values of the various composites of PANI and TANIPANI (top left: no metal oxide, top right: ZnO, bottom left: TiO_2, bottom right: Al_2O_3).

and electronic properties and exploring their potential use in solar cell applications.

References

1. Gangopadhyay, R.; De, A. Chem Mater 2000, 2, 608.
2. Hsu, J. W. P.; Lloyd, M. T. Mater Res Bull 2010, 35, 422.
3. Gunes, S.; Neugebauer, H.; Sariciftci, N. S. Chem Rev 2007, 107, 1324.
4. Hoppe, H.; Sariciftci, N. S. J Mater Res 2004, 19, 1924.
5. Qi, Y. N.; Xu, F.; Sun, L. X.; Zeng, J. L.; Lui, Y. Y. J Therm Anal Calorim 2008, 94, 553.
6. Boucle, J.; Ravirajan, P.; Nelson, J. J Mater Chem 2007, 17, 3141.
7. Mor, G. K.; Shankar, K.; Paulose, M.; Varghese, O. K.; Grimes, C. A. Appl Phys Lett 2007, 91, 152111.
8. Beek, W. J. E.; Wienk, M. M.; Janssen, R. A. J. J Mater Chem 2005, 15, 2985.
9. Taylor, K. K. Doctoral Thesis, University of Arkansas at Little Rock, 2006; p 53.
10. McDonald, M.; Mila, I.; Scalbert, A. J Agric Food Chem 1996, 44, 599.
11. Bourdo, S. E.; Saini, V.; Warford, B. A.; Prou, F.; Bairi, V.; Li, Z.; Biris, A. S.; Viswanathan, T. Mater Res Soc Symp Proc 2010, 1270, 14.
12. Mohammad, R. K.; Hyun, W. L.; In, W. C.; Sung, M. P.; Weontae, O.; Jeong, H. Y. Polym Compos 2010, 31, 83.
13. Hesheng, X.; Qi, W. Chemmater 2002, 14, 2158.
14. MacDiarmid, A. G.; Mattoso, H. C.; Manohar, S. K.; Epstein, A. J. J Polym Sci Part A: Polym Chem 1995, 33, 1227.
15. Zhang, K.; Jing, X. Polym Adv Technol 1990, 20, 689.
16. Thamaphat, K.; Limsuwan, P.; Ngotawornchai, B. J Nat Sci 2008, 42, 357.
17. Gonclaves, R. H.; Schreiner, W. H.; Leite, E. R. Langmuir. 2010, 26, 11657.
18. Arora, M.; Gupta, S. K. AIP Conf Proc 2008, 1075, 118.
19. Lee, S.-H.; Lee, D.-H.; Lee, K.; Lee, C.-W. Adv Funct Mater 2005, 15, 1495.
20. Nabid, M. R.; Golbabaee, M.; Moghaddam, A. B.; Dinarvand, R.; Sedghi, R. Int J Electrochem Sci 2008, 3, 1117.
21. Lee, S. H.; Lee, C. W. U.S. Pat. 0269555 (2005).